

University of Groningen

## Scaffold Vaccines for Generating Robust and Tunable Antibody Responses

Najibi, Alexander J.; Dellacherie, Maxence O.; Shih, Ting-Yu; Doherty, Edward J.; White, Des A.; Bauleth-Ramos, Tomás; Stafford, Alexander G.; Weaver, James C.; Yeager, Chyenne D.; Seiler, Benjamin T.

*Published in:*  
Advanced Functional Materials

*DOI:*  
[10.1002/adfm.202110905](https://doi.org/10.1002/adfm.202110905)

**IMPORTANT NOTE: You are advised to consult the publisher's version (publisher's PDF) if you wish to cite from it. Please check the document version below.**

*Document Version*  
Publisher's PDF, also known as Version of record

*Publication date:*  
2022

[Link to publication in University of Groningen/UMCG research database](#)

*Citation for published version (APA):*

Najibi, A. J., Dellacherie, M. O., Shih, T.-Y., Doherty, E. J., White, D. A., Bauleth-Ramos, T., Stafford, A. G., Weaver, J. C., Yeager, C. D., Seiler, B. T., Pezone, M., Li, A. W., Sarmento, B., Santos, H. A., Mooney, D. J., & Gu, L. (2022). Scaffold Vaccines for Generating Robust and Tunable Antibody Responses. *Advanced Functional Materials*, 32, Article 2110905. <https://doi.org/10.1002/adfm.202110905>

### Copyright

Other than for strictly personal use, it is not permitted to download or to forward/distribute the text or part of it without the consent of the author(s) and/or copyright holder(s), unless the work is under an open content license (like Creative Commons).

The publication may also be distributed here under the terms of Article 25fa of the Dutch Copyright Act, indicated by the "Taverne" license. More information can be found on the University of Groningen website: <https://www.rug.nl/library/open-access/self-archiving-pure/taverne-amendment>.

### Take-down policy

If you believe that this document breaches copyright please contact us providing details, and we will remove access to the work immediately and investigate your claim.

*Downloaded from the University of Groningen/UMCG research database (Pure): <http://www.rug.nl/research/portal>. For technical reasons the number of authors shown on this cover page is limited to 10 maximum.*

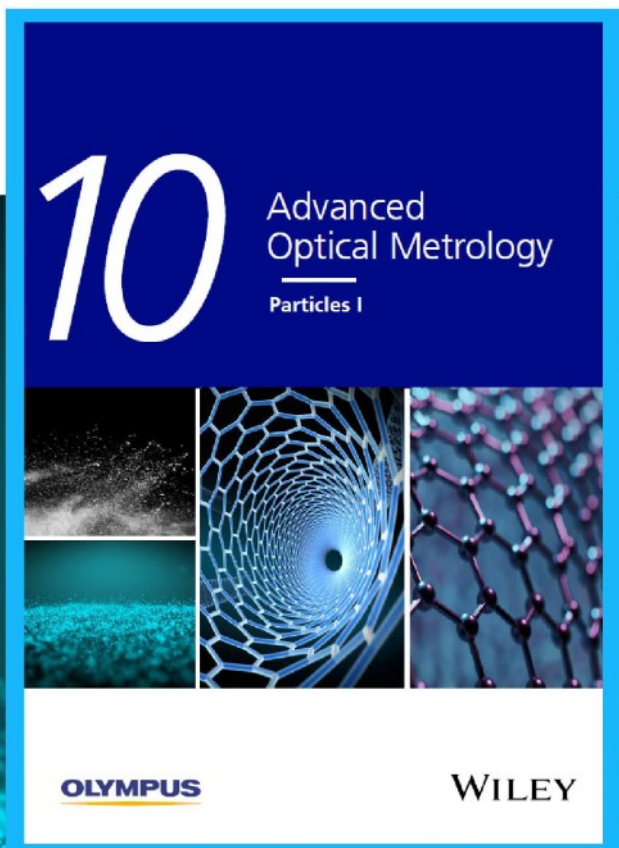


# Particles I

Access the latest eBook →

Particles: Unique Properties,  
Uncountable Applications

**Read the latest eBook and  
better your knowledge with  
highlights from the recent  
studies on the design and  
characterization of micro-  
and nanoparticles for  
different application areas.**



**Access Now**

This eBook is sponsored by

**OLYMPUS**

**WILEY**

# Scaffold Vaccines for Generating Robust and Tunable Antibody Responses

Alexander J. Najibi, Maxence O. Dellacherie, Ting-Yu Shih, Edward J. Doherty, Des A. White, Tomás Bauleth-Ramos, Alexander G. Stafford, James C. Weaver, Chyenne D. Yeager, Benjamin T. Seiler, Matthew Pezone, Aileen W. Li, Bruno Sarmiento, Hélder A. Santos, David J. Mooney,\* and Luo Gu\*

Traditional bolus vaccines often fail to sustain robust adaptive immune responses, typically requiring multiple booster shots for optimal efficacy. Additionally, these provide few opportunities to control the resulting subclasses of antibodies produced, which can mediate effector functions relevant to distinct disease settings. Here, it is found that three scaffold-based vaccines, fabricated from poly(lactide-co-glycolide) (PLG), mesoporous silica rods, and alginate cryogels, induce robust, long-term antibody responses to a model peptide antigen gonadotropin-releasing hormone with single-shot immunization. Compared to a bolus vaccine, PLG vaccines prolong germinal center formation and T follicular helper cell responses. Altering the presentation and release of the adjuvant (cytosine-guanosine oligodeoxynucleotide, CpG) tunes the resulting IgG subclasses. Further, PLG vaccines elicit strong humoral responses against disease-associated antigens HER2 peptide and pathogenic *E. coli*, protecting mice against *E. coli* challenge more effectively than a bolus vaccine. Scaffold-based vaccines may thus enable potent, durable and versatile humoral immune responses against disease.

99% from the pre-vaccine era to the mid 2000s.<sup>[1]</sup> It is estimated that from 2000 to 2019, widening vaccine access has saved over 37 million lives in low- and middle-income countries, predominantly in young children for whom the mortality rate has declined by 57%.<sup>[2]</sup>

Vaccines typically aim to trigger specific immune responses against pathogens. To do so, vaccines deliver pathogen-associated antigen, which can be formulated in several ways including live-attenuated, inactivated, toxoid, protein subunit/conjugate, viral vector, or nucleic acid.<sup>[3]</sup> For non-live (particularly subunit) vaccines, adjuvants are often co-administered to augment the immune response. Once injected, vaccine components are taken up by antigen-presenting cells (APCs) and/or drain to local draining lymph nodes (LNs) where B and T cells detect antigen and initiate the adaptive immune response.<sup>[4]</sup> Activated

follicular B cells proliferate rapidly in germinal centers (GCs), and repeated cycles of expansion and T cell-based selection generate B cells capable of producing high-affinity antibodies with isotypes dependent on the phenotype of T cell help.<sup>[5,6]</sup> For

## 1. Introduction

Vaccines are an unequivocal public health success. The advent of immunization against infectious diseases such as diphtheria, measles, smallpox, and others reduced associated deaths over

A. J. Najibi, M. O. Dellacherie, T.-Y. Shih, A. W. Li, D. J. Mooney, L. Gu  
John A. Paulson School of Engineering and Applied Sciences  
Harvard University  
Cambridge, MA 02138, USA  
E-mail: mooneyd@seas.harvard.edu; luogu@jhu.edu

A. J. Najibi, M. O. Dellacherie, T.-Y. Shih, E. J. Doherty, D. A. White,  
A. G. Stafford, J. C. Weaver, C. D. Yeager, B. T. Seiler, M. Pezone,  
A. W. Li, D. J. Mooney, L. Gu  
Wyss Institute for Biologically Inspired Engineering at Harvard University  
Boston, MA 02115, USA

T. Bauleth-Ramos, H. A. Santos  
Drug Research Program  
Division of Pharmaceutical Chemistry and Technology  
Faculty of Pharmacy  
University of Helsinki  
Helsinki FI-00014, Finland

 The ORCID identification number(s) for the author(s) of this article can be found under <https://doi.org/10.1002/adfm.202110905>.

B. Sarmiento  
Instituto de Investigação e Inovação em Saúde (i3S)  
University of Porto  
Rua Alfredo Allen, 208, Porto 4200-135, Portugal

B. Sarmiento  
CESPU  
Instituto de Investigação e Formação Avançada em  
Ciências e Tecnologias da Saúde  
Rua Central da Gandra 1317, Gandra 4585-116, Portugal

H. A. Santos  
Department of Biomedical Engineering and W.J. Kolff Institute for  
Biomedical Engineering and Materials Science  
University Medical Center Groningen/University of Groningen  
Ant. Deusinglaan 1, Groningen 9713 AV, The Netherlands

L. Gu  
Department of Materials Science and Engineering  
Institute for NanoBioTechnology  
Johns Hopkins University  
Baltimore, MD 21218, USA

DOI: 10.1002/adfm.202110905

example, type-1 T helper (Th1) CD4<sup>+</sup> T cells producing interferon gamma (IFN $\gamma$ ) can induce IgG2a class switching, while type-2 T helper (Th2) cells producing type-2 cytokines including interleukin (IL)-4 and IL-5 direct an IgG1 isotype.<sup>[7]</sup> GC-matured B cells can differentiate into plasma cells, producing high levels of antibodies, and memory cells, which potentiate long-term responses. The germinal center reaction is critical for effective humoral immunity and protection against a variety of diseases, including SARS-CoV-2.<sup>[8,9]</sup>

Despite the success of vaccination, traditional vaccine formulations present several challenges. Standard vaccines are often hindered by low magnitude and persistence of the humoral immune response, and typically require several booster shots for optimal efficacy.<sup>[3]</sup> Multi-dose vaccine schedules complicate immunization in regions with reduced healthcare access, and introduce additional pain, inconvenience, and cost.<sup>[10]</sup> The Centers for Disease Control estimate that in 2019, 5.9 million children initiated but did not complete the three-dose diphtheria-tetanus-pertussis vaccine series; these “underimmunized” children are more susceptible to mortality from preventable disease.<sup>[11]</sup> Even with the two-dose mRNA vaccines against SARS-CoV-2, a significant proportion of recipients missed the second shot, reducing the effectiveness of the vaccines and complicating the inoculation protocol.<sup>[12,13]</sup> Furthermore, standard vaccines provide little opportunity to tune the resulting antibody isotypes, which may have important implications for effector function.<sup>[14]</sup> A growing knowledge of adjuvant effects and APC subtypes provides a basis to better engineer these outcomes.<sup>[15,16]</sup> For example, the cationic polymer polyethylenimine (PEI) can control the release of negatively charged adjuvants, such as the Toll-like receptor 9 (TLR9) agonist cytosine-guanosine oligodeoxynucleotide (CpG), from biomatrices, but presents its own intrinsic immunogenicity and adjuvanticity which may affect the quality of immune response.<sup>[17,18]</sup>

Biomaterial-based vaccines can enable controlled release of antigen and adjuvant in a manner mimicking infection or multiple bolus doses, and provide a tunable platform to influence the phenotype of immune response.<sup>[19,20]</sup> Polymeric formulations, especially poly(lactide-co-glycolide) (PLG), have been heavily explored due to their biocompatibility, extensive history of safe clinical applications, and tunability of release.<sup>[21]</sup> Although these delivery vehicles have primarily been investigated in particulate form, scaffold-based vaccines that can both release biomolecules in a controlled manner and provide a niche for immune cell recruitment and education have also been explored.<sup>[22,23]</sup> Previously, porous PLG scaffolds loaded with granulocyte-macrophage colony stimulating factor (GM-CSF), CpG, and tumor antigen in the form of tumor lysates mediated control of melanoma tumors.<sup>[17,24]</sup> However, B cell and antibody responses were not characterized. More recently, a macroscale biomaterial self-assembled by inorganic mesoporous silica rods (MSR) elicited potent and long-lived GC responses and higher antibody titers than a bolus injection against various antigens, including the reproductive hormone gonadotropin-releasing hormone (GnRH), nicotine, and a cancer HER2 epitope.<sup>[25]</sup> This same material system protected mice and pigs against *E. coli*-induced sepsis, and induced strong antibody production against methicillin-resistant *Staphylococcus aureus* (MRSA) antigen.<sup>[26]</sup> These results suggest that macro-scale vaccine scaffolds may

serve as a robust and versatile platform for inducing antibody responses against a variety of target antigens.

To explore whether a scaffold vaccine strategy based on different materials systems can be broadly useful, here we fabricated three types of biomaterial scaffold vaccines (PLG, MSR, and alginate cryogel) and compared their capability to elicit antibody responses against a model antigen GnRH. GnRH is a peptide hypothalamic hormone that controls gonadotropin release and eventually spermatogenesis and ovarian follicle development. Vaccination against GnRH has been shown to reduce testosterone levels in patients with advanced prostate cancer and decrease reproductive capability in feral animals as a humane alternative to surgical castration.<sup>[27–30]</sup> Here, GnRH was conjugated to the carrier protein ovalbumin (OVA) because previous studies have shown that carrier proteins containing T-helper cell epitopes can increase antibody responses against GnRH.<sup>[25]</sup> These scaffold vaccine systems all accumulate host antigen presenting cells (APCs) and program them in situ by presenting antigens and immunostimulants to induce effective adaptive immunity (Figure S1, Supporting Information).<sup>[24,25,31,32]</sup> However, there has not been a direct comparison of their capabilities to elicit humoral immune responses. Using PLG scaffolds, we also examined whether the resultant GC formation, T follicular helper (T<sub>fh</sub>) cell responses, and IgG subclasses could be tuned by controlling the presentation and release of CpG adjuvant. In addition, the potential utility of PLG vaccines against other disease-associated antigens, HER2 peptide and a pathogenic *E. coli* strain RS218, was investigated.

## 2. Results

### 2.1. Biomaterial Scaffold Vaccines Generate Strong and Persistent Humoral Immune Responses against GnRH Peptide

To evaluate whether different scaffold vaccines targeting the same peptide antigen can induce robust antibody responses, we fabricated porous PLG scaffolds,<sup>[24]</sup> MSR vaccines,<sup>[25,31]</sup> and alginate cryogels (Cryogel),<sup>[32,33]</sup> and inoculated C57BL/6 mice (Figure S2a, Supporting Information). The three scaffold vaccines all contained the same quantity of model antigen GnRH-ovalbumin conjugate (OVA-GnRH) (Figures S3 and S4, Supporting Information, and Table 1). GM-CSF was incorporated into the three scaffold vaccines as an APC-recruiting factor, and free CpG (for MSR and Cryogel) or PEI-condensed CpG (for PLG) were used as adjuvants based on previously established formulations (Table 1).<sup>[24,25,32]</sup> Previously, it was demonstrated that PEI binds to CpG and forms nanoparticles during condensation, which slows the release of CpG from PLG scaffolds. This was found to be helpful to enhance cell-mediated immunity against melanoma tumors for PLG cancer vaccines.<sup>[17]</sup> This PLG vaccine formulation will be referred to as PEI-CpG in subsequent experiments.

All three scaffold vaccines generated robust anti-GnRH IgG1 titers that persisted over a year with a single inoculation, while a soluble bolus vaccine (without a biomaterial scaffold) containing the same quantity of antigen, CpG, and GM-CSF as the PLG vaccine induced a substantially lower IgG1 response (Figure 1a and Figure S5a, Supporting Information).

**Table 1.** Quantity of GM-CSF, CpG, and OVA-GnRH in scaffold vaccines.

Scaffold vaccine platform	APC chemoattractant (GM-CSF) [ $\mu\text{g}$ ]	Adjuvant (CpG) [ $\mu\text{g}$ ]	Antigen (OVA-GnRH) [ $\mu\text{g}$ ]
PLG, PEI-CpG	3	300	300
PLG, Free CpG	3	300	300
Cryogel (2x)	3	70	300
MSR	1	100	300

Interestingly, although the three types of scaffolds are based upon different materials, they elicited comparable levels of anti-GnRH IgG1 antibody for the majority of the 14-month study. In contrast, only the MSR and Cryogel vaccines induced robust IgG2c antibodies against GnRH, while this formulation of PLG and the bolus vaccines led to low titers of anti-GnRH IgG2c antibody (Figure 1b and Figure S5b, Supporting Information). No antibody response was detected against a negative control

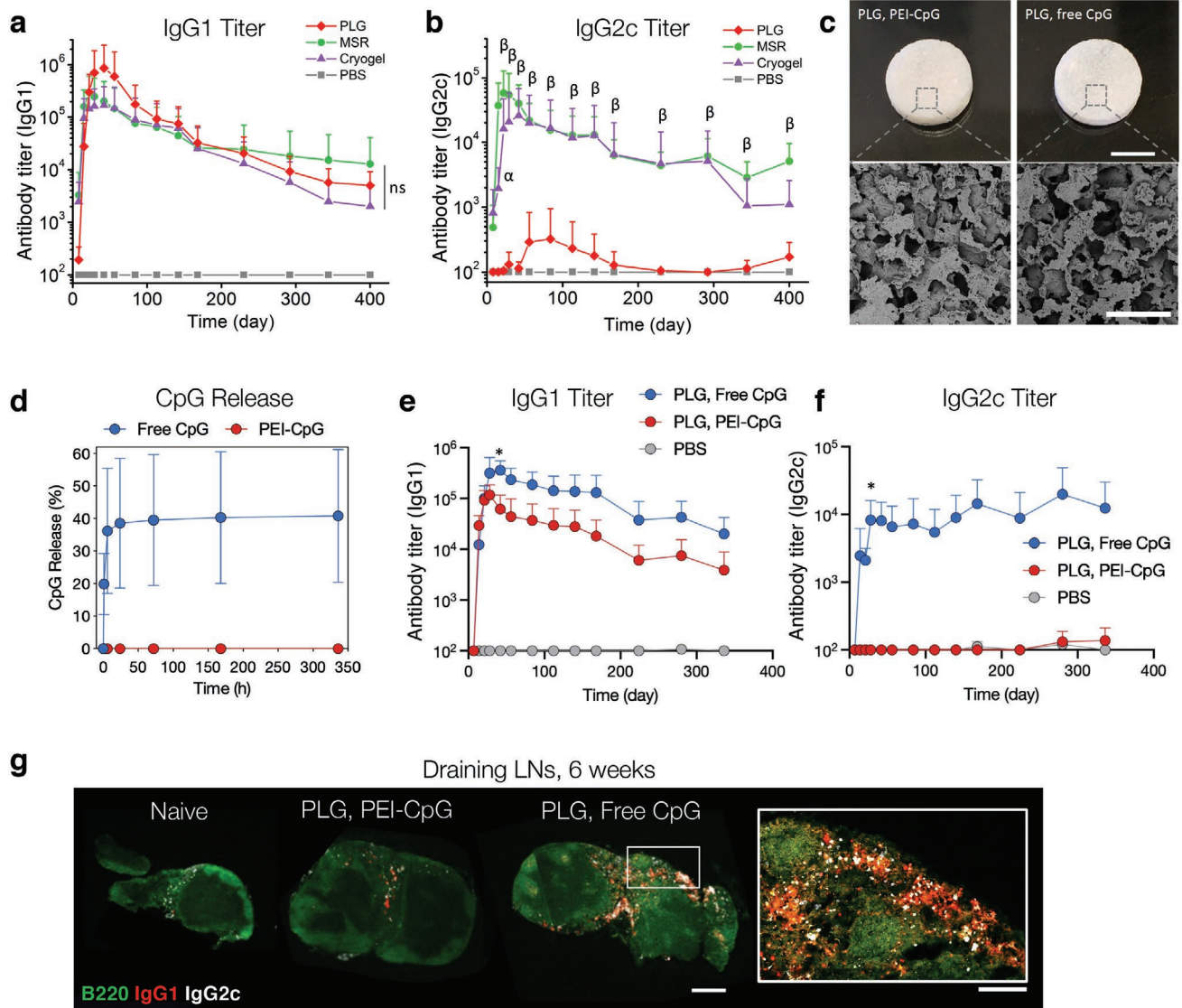


**Figure 1.** PLG vaccines generate strong and persistent humoral immune responses against GnRH peptide, with antibody subclasses dependent on CpG formulation. In (a) and (b), C57BL/6 mice were immunized with PLG, MSR, or Cryogel vaccines containing OVA-GnRH peptide and compared to PBS-injected controls. Serum was collected up to 400 d after vaccination. a) IgG1 and b) IgG2c titers against GnRH. Data represent mean  $\pm$  SD;  $n = 8$  biologically independent animals per group, sampled longitudinally. IgG1 titers are not significantly different (ns) between the three scaffold vaccine groups. For IgG2c titers in (b),  $\alpha$  indicates  $p < 0.05$  between PLG and Cryogel vaccine groups,  $\beta$  indicates  $p < 0.05$  between PLG and MSR vaccine groups. c) Photographs (above) and scanning electron microscope images (below) of PLG scaffolds containing PEI-CpG or free CpG. d) In vitro release of CpG, incorporated in free form or with PEI condensation, from PLG scaffolds. Differences are statistically significant (1 h,  $p = 0.005$ ; 6 h,  $p = 0.009$ ; 24 and 72 h,  $p = 0.008$ ; 168 and 336 h,  $p = 0.007$ ). For (e)–(g), C57BL/6 mice were immunized with PLG vaccines containing PEI-CpG or free CpG and compared to naïve controls. Serum was collected up to 336 d after vaccination. e) IgG1 and f) IgG2c titers. Data represent mean  $\pm$  SD;  $n = 5$  biologically independent animals per group, sampled longitudinally. \* indicates  $p < 0.05$  between PEI-CpG PLG vaccine group and free CpG PLG vaccine group. g) Immunohistochemistry of B220, IgG1, and IgG2c in axillary lymph nodes six weeks after vaccination. Naïve, PLG PEI-CpG, and PLG free CpG lymph nodes are depicted (left scale bar = 500  $\mu\text{m}$ ) and higher magnification of a free CpG lymph node (different section of the same node, right scale bar = 150  $\mu\text{m}$ ).

protein (BSA) not delivered in the vaccines (Figure S6a,b, Supporting Information). It should be noted that IgG2a (expressed by some mouse strains such as BALB/c) is replaced by the allelic variant IgG2c in certain mouse strains such as C57BL/6, NOD, and SJL. IgG2a and IgG2c are generally considered to have equivalent function.<sup>[34–36]</sup>

To investigate whether differences in CpG presentation and release contributed to the minimal IgG2c antibody production in C57BL/6 mice treated with the PLG vaccine, PLG vaccines incorporating either free or PEI-condensed CpG were next compared. Altering the form of incorporated CpG did not affect the scaffold structure, antigen incorporation or release profile, but markedly changed the release kinetics of CpG (Figure 1c,d; Figure S7a,b, Supporting Information). C57BL/6 mice inoculated with PLG vaccines containing either free or PEI-CpG exhibited a robust anti-GnRH IgG1 response, with high titers persisting over the course of the study for both groups (Figure 1e). While the PLG with PEI-CpG again induced low IgG2c titers, the free CpG PLG vaccine elicited a strong IgG2c response that persisted over ten months (Figure 1f). Vaccine-draining inguinal LNs were harvested at six weeks post-vaccination and stained for IgG1 and IgG2c. Consistent with serum titers, immunohistochemistry of inguinal LNs from mice treated with the PLG free CpG vaccine group showed a much stronger IgG2c signal than the PLG vaccine with PEI-CpG (Figure 1g).

## 2.2. PLG Vaccines Elicit Durable Germinal Center and T<sub>fh</sub> Responses

To examine potential mechanisms underlying the observed differences in antibody response between vaccine formulations, C57BL/6 mice were implanted with PLG scaffolds containing OVA-GnRH, GM-CSF, and free or PEI-condensed CpG, or injected with a soluble bolus vaccine, and GC development was compared to naïve controls (Figure S2b, Supporting Information; Figure 2a). In axillary nodes, naïve mice showed no GC activation, while all three vaccine groups demonstrated GC formation by two weeks (Figure S8, Supporting Information). By six weeks, GC activity was only observed in mice implanted with PLG scaffolds, most strikingly in the free CpG PLG group (Figure 2b, Figure S9, Supporting Information). In inguinal LNs, GCs were detected in PLG vaccine groups by two weeks, and were maintained to six weeks in mice treated with the free CpG vaccine (Figure S9, Supporting Information). Compared to naïve mice, LNs from vaccinated mice had increased numbers of total cells and B cells, which declined between one and six weeks, and were most significantly elevated with the free CpG PLG vaccine (Figure S10a,b, Supporting Information). Analysis of the number of GL7<sup>+</sup> peanut agglutinin (PNA)-expressing B cells revealed elevated numbers only in PLG conditions, as early as one week after immunization (Figure 2c; Figure S11, Supporting Information). GC B cells peaked at two weeks, and only the free CpG PLG vaccine maintained a significant increase after three weeks. CD4<sup>+</sup> T cell numbers in LNs of vaccinated mice peaked at day seven, subsequently declined, and were significantly elevated only in the PLG vaccine with free CpG (Figure S10c, Supporting Information). Numbers of

CXCR5<sup>+</sup>PD-1<sup>+</sup> T<sub>fh</sub> cells increased in both PLG vaccine groups out to two weeks (Figure 2d; Figure S11, Supporting Information). Notably, only the free CpG PLG vaccine sustained this response three weeks post-immunization. The proportions of T<sub>fh</sub> and GC B cells in PLG were similarly elevated at later time-points (>2 weeks) compared to naïve mice, but not bolus-vaccinated mice (Figure S12a,b, Supporting Information).

## 2.3. PLG Formulation Can Bias toward a Th1-Type Immune Response

To determine if the elevated IgG2c titer observed with the free CpG PLG vaccine resulted from an elevated Th1-type response,<sup>[6,37]</sup> cytokine levels at the vaccine site and draining lymph node were characterized. Analysis of explanted PLG vaccines containing free or PEI-CpG revealed high concentrations of GM-CSF, TNF $\alpha$ , and IL-12p70, among other cytokines, indicative of immune activation (Figure S13, Supporting Information). Notably, PLG vaccines with PEI-CpG had elevated concentrations of Th2-type cytokines compared to PLG with free CpG (Figure 2e). PLG vaccines with PEI-CpG induced a robust IL-5 response at the earliest time point, which declined over time, followed by a rise in IL-10 which remained significantly higher out to six weeks than in the free CpG vaccine group.

To investigate whether the Th2-type response could be due to the controlled slow release of CpG, or the presence of PEI itself, C57BL/6 mice were implanted with PLG scaffolds that contained either no adjuvant, PEI alone, or PEI + CpG both in a free form (i.e., not condensed together). In the latter, PEI and CpG were loaded into PLG vaccines separately and in lyophilized form; through this approach, rapid CpG release was decoupled from the presence of PEI. Without GM-CSF and antigen in the scaffolds, no IL-5 response was detected (Figure S14a, Supporting Information). With the addition of GM-CSF and OVA, PLG vaccines containing no adjuvant induced an intermediate IL-5 response, which was enhanced with PEI, and abrogated with the inclusion of free CpG (Figure 2f).

Finally, LNs and spleens were collected from these mice and stained for Th1 and Th2-type transcription factors (Tbet and GATA3, respectively) in CD4<sup>+</sup> T cells. PLG vaccines containing free CpG induced stronger Th1-type CD4<sup>+</sup> T cell responses compared to PLG vaccines with PEI alone (Figure 2g). Such differences were not observed without GM-CSF and antigen in the vaccines (Figure S14b, Supporting Information). These data suggest that the IgG2c response in the free CpG PLG vaccine is due to reduced Th2-type cytokines in the vaccine site as a result of rapid CpG release, leading to systemic Th1-type immunity against the vaccine antigen.

## 2.4. Free CpG PLG Vaccine Improves Humoral Response against HER2<sup>+</sup> Breast Cancer and RS218 Infection

The ability of PLG vaccines to generate humoral responses against HER2<sup>+</sup> cancer was next assessed. PLG vaccines were loaded with GM-CSF, free or PEI-condensed CpG, and antigen in the form of a peptide from the Trastuzumab-binding domain of HER2 linked to a CD4<sup>+</sup> T cell epitope from measles virus

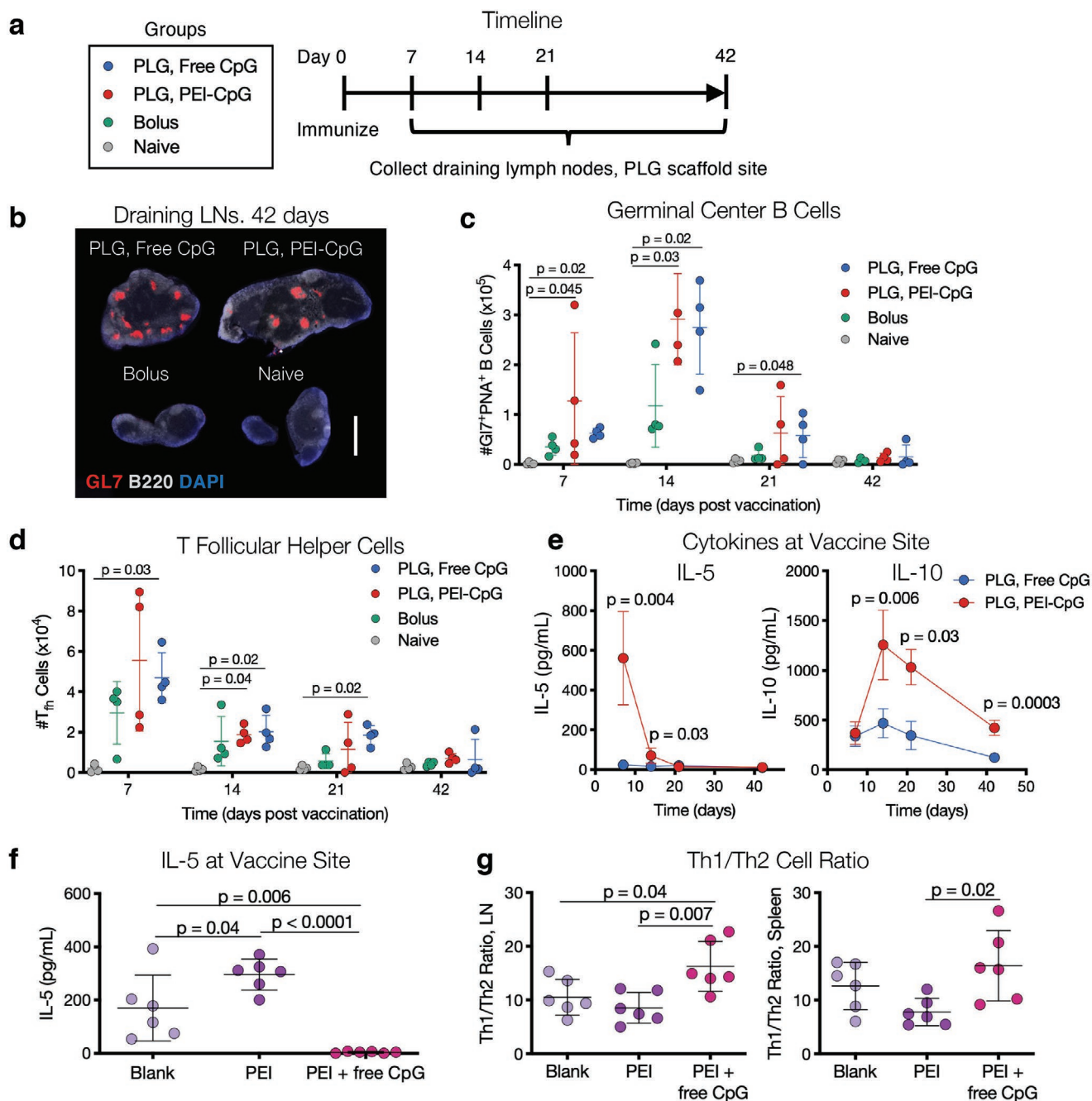


**Figure 2.** Free CpG PLG vaccines promote durable germinal center activation, T<sub>fh</sub> response, and Th1-type immunity. a) Experimental timeline and vaccine conditions. C57BL/6 mice were immunized with PLG (PEI-CpG or free CpG) or bolus vaccines containing OVA-GnRH on day 0, and compared to naïve controls. Draining lymph nodes and the PLG scaffold site were collected 7, 14, 21, and 42 d after vaccination. b) Immunohistochemistry of axillary lymph nodes to assess germinal centers six weeks after immunization. Scale bar = 1 mm. Flow cytometry analysis of c) germinal center B cells (B220<sup>+</sup> GL7<sup>+</sup> peanut agglutinin<sup>+</sup>) and d) T follicular helper cells (CD3<sup>+</sup> CD4<sup>+</sup> CXCR5<sup>+</sup> PD-1<sup>+</sup>) within pooled axillary and inguinal lymph nodes. e) Concentrations of cytokines IL-5 (left) and IL-10 (right) within tissues formed in PLG scaffolds. For (c)–(e), data represent mean ± SD; n = 4 biologically independent animals per group per timepoint. f, g) C57BL/6 mice were immunized with PLG scaffolds containing no adjuvant (Blank), PEI alone, or PEI + CpG in a free form (not condensed), and scaffolds, lymph nodes, and spleens were extracted after 7 d. f) Concentration of IL-5 in scaffolds and g) ratio of Th1 (Tbet<sup>+</sup>) to Th2 (GATA3<sup>+</sup>) CD4<sup>+</sup> T cells in lymph nodes (left) and spleens (right). Data represent mean ± SD; n = 6 biologically independent animals per group.

fusion protein (MVF-HER2), as developed in previous studies (Figure 3a,b).<sup>[25,38]</sup> The different CpG formulations did not alter MVF-HER2 loading in PLG vaccines (Figure S15, Supporting Information). Both formulations of the PLG vaccine elicited

strong anti-HER2 IgG1 titers in BALB/c mice (Figure 3c). Consistent with the prior IgG2c results in the C57BL/6 OVA-GnRH model, here the free CpG PLG vaccine increased anti-HER2 IgG2a titers compared to the PEI-CpG formulation (Figure 3d).

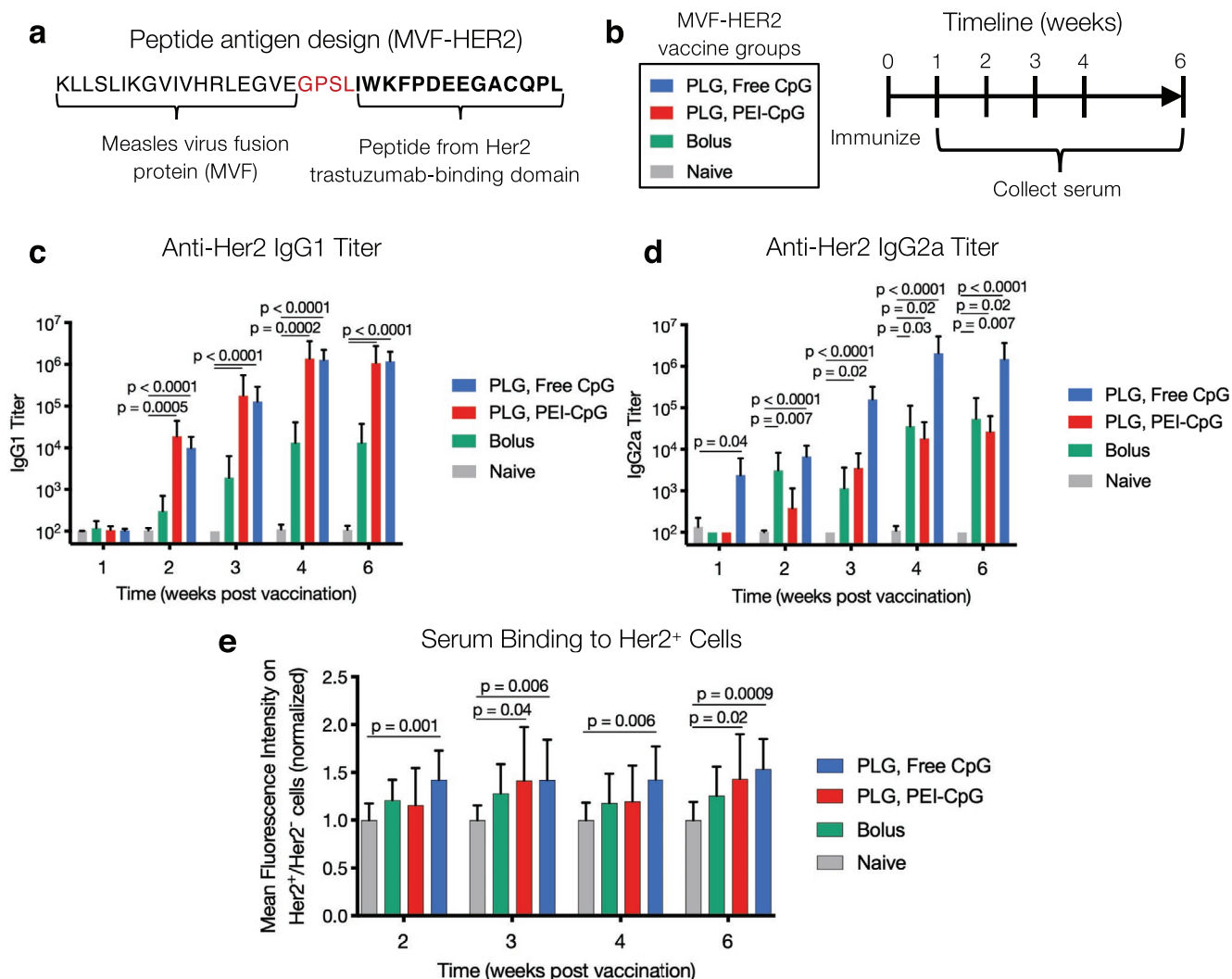


**Figure 3.** PLG vaccines elicit humoral responses against HER2. a) Design of the peptide antigen to target HER2. b) Schematic of the experimental timeline. BALB/c mice were immunized with PLG (PEI-CpG or free CpG) or bolus vaccines containing MVf-HER2 and compared to naïve controls. c) IgG1 and d) IgG2a antibody titers against HER2. e) Binding of serum from immunized or control mice to HER2<sup>+</sup> breast cancer cells. Data represent mean  $\pm$  SD;  $n = 10$  biologically independent animals per group.

To determine whether these antibodies could recognize HER2 antigen, their capacity to bind cancer cells expressing HER2 receptors was examined. Serum antibodies from vaccinated mice bound HER2<sup>+</sup> (TUBO) more strongly than HER2<sup>-</sup> (4T1) cancer cells, and mice treated with the PLG free CpG vaccine showed increased serum binding to HER2<sup>+</sup> cells at all timepoints investigated (Figure 3e; Figure S16, Supporting Information).

We next investigated the vaccines' ability to induce immunity against a pathogenic *E. coli* strain RS218, originally isolated from a human neonate with meningitis.<sup>[39,40]</sup> BALB/c mice were vaccinated with PLG vaccines containing GM-CSF, microbead-immobilized RS218 lysate antigen, and either free or PEI-condensed CpG, and then challenged with an intraperitoneal injection of the pathogen 28 d after vaccination (Figure 4a). The bolus vaccine and both PLG vaccine formulations induced

antibody responses against RS218, but only the free CpG PLG vaccine elicited a significantly higher IgG titer than the naïve control at four weeks post vaccination (Figure 4b). After RS218 challenge, none of the unvaccinated (naïve) animals survived (Figure 4c). About two-third of the mice inoculated with the bolus vaccine survived the lethal RS218 challenge. Over 80% of the mice survived the challenge when immunized with PLG vaccines containing PEI-CpG, consistent with prior investigation in this infection model.<sup>[26]</sup> Strikingly, the free CpG PLG vaccine was able to protect 100% of the mice. Post-mortem quantification of bacteria within isolated organs revealed that mice immunized with PLG vaccines had significantly lower bacterial counts in the lung, liver, kidney, and spleen than the naïve mice (Figure 4d). In addition, free CpG PLG vaccination reduced these numbers by  $\approx 10^1$ – $10^4$  as compared to vaccination with PLG containing PEI-CpG or bolus vaccines.

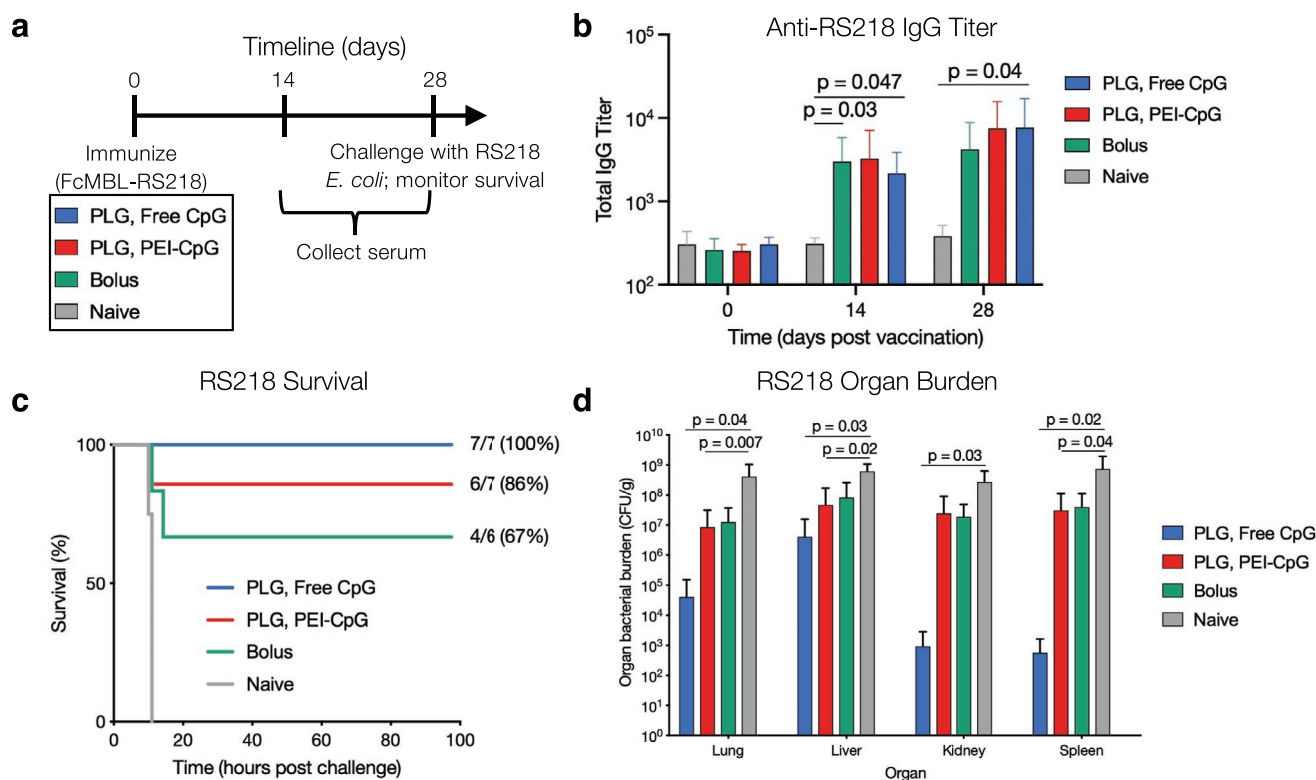


**Figure 4.** Prophylactic free CpG PLG vaccine protects against infectious disease. a) Schematic of the experimental timeline. BALB/c mice were immunized with PLG (PEI-CpG or free CpG) or bolus vaccines containing microbead-immobilized RS218 lysate and compared to naïve controls. Mice were challenged with RS218 *E. coli* 28 d after immunization. b) Total IgG antibody titer against RS218 *E. coli*. Data represent mean  $\pm$  SD;  $n = 6$  (vaccines) or 4 (naïve) biologically independent animals per group. c) Survival and d) endpoint organ bacterial burden of mice challenged with RS218 *E. coli*. Data represent mean  $\pm$  SD;  $n = 8$  (vaccines) or 6 (naïve) biologically independent animals per group.

### 3. Discussion

The three scaffold vaccines studied here (PLG, MSR, and Cryogel) all elicited strong humoral immune responses, with anti-GnRH antibody titers orders of magnitude higher than those generated by a bolus vaccine (Figure 1a,b; Figure S5, Supporting Information). Strikingly, these robust antibody titers persisted more than a year with a single immunization. It has previously been demonstrated that systems which deliver antigen in a sustained manner, mimicking natural infections, improve GC responses.<sup>[20,41]</sup> The scaffold-based vaccines studied here, which all continually release OVA coupled peptide antigens on the order of weeks, likely continue to supply antigen to LNs when GC activity and high-affinity IgG production have been initiated.<sup>[42]</sup> These findings suggest one may in the future select vaccine material platforms based on desired physical or chemical properties instead of only their immunogenicity. For example, one may choose PLG scaffolds because of their biodegradability and safety record in clinical applications, or MSR for their injectability and ease of preparation.

A significant difference in antibody subclass profile in PLG vaccines was found with the distinct CpG formulations (Figure 1f). Relative to the free CpG PLG vaccine, PLG vaccines containing PEI induced type-2 cytokines (e.g., IL-5 and IL-10) and a Th2-biased immune response (Figure 2e–g). Because no IL-5 was detected in PLG scaffolds lacking GM-CSF or

antigen, the cells recruited to the vaccine site through GM-CSF likely contribute to this cytokine signaling (Figure S14a, Supporting Information). We propose that mechanistically, PEI in the PEI-CpG PLG vaccine drives local type-2 cytokine signaling (both intrinsically and by slowing the release of CpG), pushing CD4<sup>+</sup> T cells to a Th2 phenotype and skewing GC B cells away from IgG2a/c. However, free CpG can promote a type-1 immune response and IgG2a/c production. These differences may have profound impacts on vaccine functionality, given the different effector functions of IgG subclasses.<sup>[14]</sup> For example, the IgG2a/c subclass in mice binds all activating Fc-gamma receptors, and mediates complement activation and antibody-dependent cellular cytotoxicity (ADCC) and phagocytosis, critical to resisting viral and bacterial infection.<sup>[36,37,43,44]</sup> Our findings may provide new strategies to control and tune the elicited antibody subclasses without fundamentally altering vaccine design.

A variety of mechanisms could underlie these findings and present opportunities for additional investigation. For example, the relative release rates of antigen and adjuvant could influence vaccine outcomes. It was previously demonstrated that rapid (compared to slow) release of a TLR7/8 agonist from a depot vaccine induced poorer IgG1 and IgG2c responses in immunized mice.<sup>[45]</sup> In our work, faster CpG release from PLG vaccines instead increased IgG2a/c antibody titers. This difference could potentially be due to the choice of TLR agonist, as free CpG can

induce TLR9 signaling in B cells and promote IgG2a/c production.<sup>[37,46]</sup> It is also possible that the differential CpG release affected early immune cell recruitment and cytokine/chemokine profiles in the vaccine microenvironment, which could impact the lymph node response. Additional studies to elucidate cellular dynamics in PLG vaccines would likely support our understanding of the antibody outcomes. Furthermore, the use of PEI to control CpG release presents an additional consideration, as PEI has been used as a vaccine adjuvant capable of improving DC antigen presentation, mixed-Th1/Th2 responses, and IgG antibody titers.<sup>[18,47–49]</sup> PEI has also been shown to stimulate type-2 immunity and secretion of IL-5 and IL-10, among other cytokines.<sup>[49–51]</sup> These reports are broadly consistent with our finding that PLG scaffolds containing GM-CSF, OVA, and PEI alone (without CpG) induced an IL-5, Th2-biased response (Figure 2f,g). Moreover, vaccination against glycoprotein antigens using PEI alone as an adjuvant led to higher IgG1/IgG2a antibody ratios than with CpG alone or PEI complexed with CpG.<sup>[47,49]</sup> These results support the observed bias of PEI-containing PLG vaccines toward IgG1 responses in our work, where we expect that PEI provides both immunogenicity and a means of controlling CpG release. It is likely that PEI-sequestered CpG remains accessible to infiltrating cells, based on prior reports of cellular activation within PEI-CpG PLG vaccines.<sup>[17]</sup> Additional studies to pinpoint the adjuvant role of PEI in the PLG vaccine microenvironment would support a mechanistic understanding of the observed differences in antibody profiles.

In both the PEI-CpG and free CpG PLG vaccine groups, robust GC responses remained detectable up to six weeks after vaccination, significantly longer than the bolus vaccine. However, only the mice treated with free CpG PLG vaccines showed significantly elevated GC B cell and  $T_{H1}$  cell numbers at three weeks compared to the naïve group (Figure 2c,d). Although  $GL7^{+}PNA^{+}$  (GC) B cell numbers in the PLG vaccine groups had declined by six weeks with flow cytometry analysis, persistent GC activity was detected at this time through a GL7 stain in the axillary lymph nodes (Figure S8, Supporting Information). It is possible that the more restrictive identification of GC B cells through flow cytometry ( $B220^{+} GL7^{+}PNA^{+}$ ) versus immunohistochemistry/IHC ( $B220^{+} GL7^{+}$ ) resulted in this difference. Additionally, the flow cytometry experiments were conducted on pooled axillary and inguinal lymph nodes, and it is likely that the two nodes did not receive equal drainage from the PLG vaccine site (Figure S2b, Supporting Information). IHC analysis, conducted separately, found that GC activity was maintained longer in the axillary than inguinal lymph nodes, suggesting this may be the case (Figures S8 and S9, Supporting Information). Labeling studies to trace the path of drainage from scaffold-based vaccines could identify which LNs serve as the primary drainage sites.<sup>[52]</sup> Broadly, the maintenance of GC activity to later timepoints is consistent with prior reports in depot-based vaccines, including the MSR system explored in this work.<sup>[25,53]</sup> Altogether, the robust and long-lived GC response likely contribute to the enhanced and persistent antibody generation, and are important for future applications of this biomaterial-based system. For example, high-affinity antibodies and GC activation are critical in effective SARS-CoV-2 response.<sup>[8,9]</sup>

PLG vaccines elicited robust humoral responses against the cancer-associated antigen HER2 (Figure 3) and conferred

protection against pathogenic *E. coli* RS218 (Figure 4). Against HER2, only the free CpG PLG vaccine improved IgG2a titers over the bolus, along with binding HER2<sup>+</sup> cancer cells over HER2<sup>-</sup> controls. Trastuzumab, a HER2-targeting monoclonal antibody, has an extensive clinical history targeting HER2<sup>+</sup> breast cancers, but presents several challenges including cost, need for repeated dosing, biodistribution, and cardiotoxicity.<sup>[38,54]</sup> Induction of strong anti-HER2 antibody responses through single-dose PLG vaccination could overcome many of these concerns. Furthermore, an IgG2a-based antibody response against HER2 could support elimination of HER2<sup>+</sup> cancer cells through an ADCC-dependent mechanism.<sup>[54–57]</sup> In the RS218 *E. coli* model, only the free CpG PLG vaccine elicited a significantly higher IgG titer than the naïve control. However, the RS218 bolus vaccine also induced high titer in this model, which may potentially be attributed to its highly immunogenic antigen; in contrast to endogenous GnRH antigen, pathogen-associated molecular patterns (PAMPs) are known to activate innate immunity and B cell responses.<sup>[58–60]</sup> Nevertheless, the PLG vaccines were still more effective in providing immune protection against RS218. A single inoculation with free CpG PLG vaccine was able to achieve complete protection against the RS218 challenge and significantly decrease bacterial loads in various organs. Taken together, these results demonstrate the advantages of the scaffold vaccine strategy in eliciting robust, functional humoral responses against cancer and infectious disease.

## 4. Conclusion

Overall, these results highlight the advantages of biomaterial scaffold vaccines for producing robust humoral immunity. During pandemics such as COVID-19, multi-dose vaccine schedules can complicate the vaccination process and cause missed shots, which may delay reaching optimal immunity and reduce vaccine effectiveness.<sup>[12,13]</sup> The scaffold vaccine strategy may help to overcome such limitations. Further, the ability to tune the antibody subclass by simply modulating the release of adjuvant from scaffold-based vaccines may achieve more precise control of the humoral immune response. Additional studies may consider the use of scaffold-based vaccines to elicit antibody isotypes other than IgG, which was primarily investigated here. In addition, exploration of alternative adjuvants and mechanisms of their controlled release may expand the antibody subclass tunability afforded by scaffold-based vaccines. Better understanding the influence of vaccine adjuvant presentation and release on human immune responses would support translation of this strategy, and could suggest relevant therapeutic contexts for its application. The ability of the PLG vaccines to produce robust humoral responses against various types of antigens, ranging from an endogenous hormone peptide to a tumor-associated antigen and bacterial lysate, indicates a potentially broad utility of biomaterial scaffold vaccines.

## 5. Experimental Section

**PLG Vaccine Fabrication:** PLG vaccines were formed as previously described.<sup>[17]</sup> Briefly, 18 mg of  $\approx 30 \mu\text{m}$  85:15 PLG microspheres containing

GM-CSF (Phosphorex #LG30-8515-MGMC) per scaffold were mixed with adjuvant and antigen, frozen in liquid nitrogen, and lyophilized. In free CpG vaccines, CpG-ODN 1826 (5'-TCCATGACGTTCTGACGT-3', Integrated DNA Technologies) was added directly. In PEI-CpG vaccines, polyethyleneimine (Millipore Sigma #P3143) was condensed with CpG in a 7:1 charge ratio: CpG solution was added dropwise into a vortexing PEI solution and rested before adding a 50% sucrose solution. OVA-GnRH was prepared by reducing cysteine-GnRH peptide (CEHWSYGLRP, Peptide 2.0) with twofold molar excess TCEP Bond Break solution (0.5 M, Pierce, VWR #PI77720). Separately, OVA protein (Invivogen Endofit) was reacted with 30-fold molar excess sulfosuccinimidyl 4-(N-maleimidomethyl)cyclohexane-1-carboxylate (sulfo-SMCC, Pierce #22322), purified with desalting columns, and then mixed overnight with reduced C-GnRH prior to desalting again (ZebaSpin 7K MWCO, Fisher #89883). MVF-HER2 antigen was prepared in a similar manner. In RS218 studies, Dyabead MyOne (Thermo Fisher Scientific) conjugated with biotinylated Fc-mannose-binding lectin captured 15 PAMP units of *E. coli* lysate for antigen as previously described.<sup>[26]</sup> After lyophilization of PLG, antigen, and adjuvant, 130 mg sieved sucrose ( $\approx 250\text{--}425\ \mu\text{m}$ ) was added per vaccine as a porogen and mixed vigorously. The mixture was compression molded at 1500 psi for 45 s into 8 mm discs using a Carver Press (Model 3850). Discs were placed in a pressure vessel and exposed to 800 PSI CO<sub>2</sub> overnight before storage at  $-20\ ^\circ\text{C}$ .

**Cryogel Vaccine Fabrication:** Ultrapure MVG sodium alginate was purchased from NovaMatrix (Sandvika, Norway) and methacrylated using 2-(N-Morpholino)ethanesulfonic acid hydrate (MES), sodium chloride (NaCl), N-(3-dimethylaminopropyl)-N'-ethylcarbodiimide hydrochloride (EDC), N-hydroxysuccinimide (NHS), hydroquinone (all purchased from Sigma-Aldrich; Atlanta, GA) and 2-aminoethyl methacrylate hydrochloride (AEMA; Polysciences; Warrington, PA) as previously reported.<sup>[32]</sup> Briefly, MVG alginate was dissolved to 0.6% wt vol<sup>-1</sup> in MES buffer (0.1 M MES, 0.3 M NaCl, pH  $\approx 6.5$ ) with 0.05 mg mL<sup>-1</sup> hydroquinone. Per 1.2 g alginate, 3.36 g EDC and 1.56 g NHS were added and mixed before adding 2.688 g AEMA. The mixture was stirred at room temperature for 17 h; MA-alginate was then precipitated in 10 $\times$  excess ethanol, collected, and dried in a vacuum chamber for 1–2 d. To prepare cryogels, MA-alginate was dissolved to 1.5% (wt vol<sup>-1</sup>) in DI water and GM-CSF (PeproTech; Rocky Hill, NJ), CpG, and OVA-GnRH were incorporated. The MA-alginate solution was mixed with 0.5% wt vol<sup>-1</sup> N,N,N',N'-tetramethylethylenediamine (Sigma) and cooled at 4  $^\circ\text{C}$  for 10 min before adding 0.25% wt vol<sup>-1</sup> ammonium persulfate (Sigma). The mixture was quickly pipetted into cold Teflon molds and frozen at  $-20\ ^\circ\text{C}$  overnight. The next day, cryogels were thawed and soaked in a bath containing 200  $\times 10^{-3}$  M calcium chloride (Sigma) and 50  $\times 10^{-3}$  M 4-(2-hydroxyethyl)-1-piperazineethanesulfonic acid (HEPES, Sigma) (pH 7.1) for 10 min. Gels were placed into a 16G needle and attached to a 1 mL syringe loaded with 250  $\mu\text{L}$  PBS for injection.

**MSR Vaccine Fabrication:** MSR vaccines were prepared as previously described.<sup>[25,31]</sup> In brief, 4 g of Pluronic P123 surfactant (average  $M_n \approx 5800$ , Sigma) was dissolved in 150 g of 1.6 M HCl, mixed with 8.6 g tetraethyl orthosilicate (TEOS, Sigma) at 40  $^\circ\text{C}$  for 20 h, and stirred at 100  $^\circ\text{C}$  for another 24 h. Pluronic P123 was removed in 1% ethanol in HCl at 80  $^\circ\text{C}$  for 18 h and MSRs were filtered and dried at 65  $^\circ\text{C}$ . To prepare MSR vaccines, 4 mg of MSRs were dissolved in PBS; 2 mg each was incubated with OVA-GnRH or CpG and shook for 8 h at room temperature before lyophilization. The next day, 1 mg of MSRs were loaded with GM-CSF for 1 h at 37  $^\circ\text{C}$  while shaking. The MSR mixtures were dissolved in PBS and combined before injection.

**Bolus Vaccines:** CpG, GM-CSF, and the relevant antigen (OVA-GnRH, MVF-HER2, or microbead-immobilized RS218 lysate) were mixed in PBS to obtain a total volume of 150  $\mu\text{L}$  per dose.

**Animal Studies:** All animal studies were performed in accordance with guidelines set by the National Institutes of Health and Harvard University Faculty of Arts and Sciences' Institutional Animal Care and Use Committee (IACUC). Prior to implantation, PLG vaccines were leached in 10 mL DI H<sub>2</sub>O until floating ( $\approx 4$  h) to remove porogen, then rinsed in 70% ethanol and sterile PBS. Vaccines were surgically

implanted subcutaneously on the left flank. 6-to-8-week old, female C57BL/6J or BALB/c mice purchased from Jackson Laboratory (Bar Harbor, ME) were used in OVA-GnRH and MVF-HER2 immunization experiments, respectively. 8-to-10-week old, male and female BALB/c mice purchased from Charles River Labs (Wilmington, MA) were used in RS218 *E. coli* vaccination experiments.

**SEM Imaging:** Structural analysis of the PLG vaccines was performed using scanning electron microscopy (SEM). The scaffolds were first leached in DI H<sub>2</sub>O for  $\approx 4$  h, rinsed in ethanol, and dried under vacuum for at least 2 d. The scaffolds were then attached to aluminum pin mounts using conductive carbon tape, sputter-coated with gold, and imaged with a Tescan Vega GMU SEM at an accelerator voltage of 20 keV.

**Antigen Loading Quantification:** After porogen leaching, PLG scaffolds were completely digested in 1 M NaOH overnight and neutralized with HCl. OVA-GnRH or MVF-HER2 in the digestion solution was then quantified using a standard micro-BCA assay (Pierce, Thermo Fisher Scientific #23235). For Cryogels, the gels were dissolved in alginate lyase solution (Sigma) overnight. OVA-GnRH or MVF-HER2 was then quantified using micro-BCA assay (Pierce, Thermo Fisher Scientific #23235).

**Release Quantification:** After porogen leaching, PLG scaffolds were incubated in PBS at 37  $^\circ\text{C}$  on a shaker and solution was periodically collected and replaced. To assess CpG release, samples were incubated with a 3.2 mg mL<sup>-1</sup> heparin solution and flowed through an XTerra MS C18 column (Waters #186000494) on an Agilent High Performance Liquid Chromatography (HPLC) 1100 system. Mobile phase consisted of 0.1 M triethylammonium acetate (TEAA, EMD Millipore #625718) and 10% 0.1 M TEAA/90% acetonitrile (J.T. Baker #JT9012-3). CpG was quantified relative to a standard curve of known concentrations ( $R^2 > 0.99$ ). At endpoint, scaffolds were digested by shaking with DMSO overnight and centrifugation to collect supernatant. To assess OVA-GnRH release, total protein was quantified using a standard micro-BCA assay (Thermo Fisher). At endpoint, scaffolds were digested by shaking with 1 M NaOH overnight, neutralization with 2 M HCl, and centrifugation to collect supernatant.

**Antibody ELISAs:** Peripheral blood was collected from mice following vaccination, coagulated for 30 min at room temperature and centrifuged at 2200 $\times$ g for 10 min to separate serum. High-binding 96-well plates (Costar 2592, Corning-Costar #EW-13020-00) were coated overnight at 4  $^\circ\text{C}$  with 30  $\mu\text{g mL}^{-1}$  of GnRH or HER2 peptide in Dulbecco's phosphate-buffered saline (DPBS, pH 7.4). Alternatively, wells were functionalized with mannose-binding lectin 2 protein (Sino Biological Inc. #10405-HNAS-50) binding RS218 *E. coli* lysate for relevant experiments. Wells were blocked with ELISA diluent (BioLegend #421203) and incubated with serum at a range of dilutions. Respective wells were incubated with biotin-anti-mouse IgG1 (BD Biosciences #550331) or IgG2a (BD Biosciences #553388) followed by streptavidin-HRP (BD Biosciences #554066) and TMB substrate (BioLegend #421101). The R19-15 antibody clone (BD Biosciences #553388) was used to detect mouse IgG2a (for BALB/c mouse experiments) and IgG2c (for C57BL/6J experiments) according to the vendor's document and published studies.<sup>[61,62]</sup> It does not react with other Ig isotypes. Plates were aspirated, washed 3 $\times$  with 0.1% Tween in DPBS, and blotted dry between steps. Absorbance was measured at 450 nm, subtracting background at 540 nm.

**Immunohistochemistry of Germinal Centers:** After vaccination, mice were euthanized at pre-defined timepoints and vaccine-draining axillary and inguinal lymph nodes were collected (one mouse per group per timepoint to supplement the flow cytometry studies). Lymph nodes were fixed in paraformaldehyde, equilibrated in 30% sucrose, and embedded in molds in Tissue-Tek OCT (VWR) to produce 20  $\mu\text{m}$  cryo-sections that were stored at  $-20\ ^\circ\text{C}$ . Sections were blocked in natural goat serum (Fitzgerald #88R-NG001) and bovine serum albumin, then stained with FITC-conjugated anti-CD45R/B220 (BioLegend #103206), biotin-conjugated anti-GL7 (BioLegend #144616), Alexa Fluor 647-conjugated anti-mouse IgG1 (Invitrogen #A21240), and/or biotin-conjugated anti-mouse IgG2a (BioLegend #407103). The RMG2a-62 antibody clone used here (BioLegend #407103) reacts with IgG2a and IgG2c in BALB/c and C57BL/6 mice, respectively, per the manufacturer. When relevant, samples were incubated with AlexaFluor 594-conjugated streptavidin

(Invitrogen #S32356). Stained sections were mounted with ProLong Gold Antifade Mountant with DAPI (Invitrogen #P36931) and imaged on a Zeiss 710 Confocal system.

**Flow Cytometry of Germinal Centers and T Helper Responses:** Spleens and vaccine-draining lymph nodes were collected and digested to obtain single-cell suspensions. Following standard flow cytometry protocols, cells were blocked with anti-CD16/CD32 (eBiosciences #14-0161-81) and stained with FITC-conjugated anti-CD45R/B220 (eBiosciences #11-0452-82), Alexa Fluor 647-conjugated anti-GL7 (BioLegend#144606), rhodamine-conjugated Peanut Agglutinin (Vector Laboratories #RL-1072), PE/Cy7-conjugated anti-CD3e (BioLegend #100320), APC-conjugated anti-CD279/PD-1 (BioLegend #135209), eFluor 450-conjugated anti-CD4 (eBiosciences #48-0042-82), PE-conjugated CXCR5 (BD Biosciences #551959), Alexa Fluor 647-conjugated anti-Tbet (BioLegend #644804), AlexaFluor 488-conjugated GATA3 (BioLegend #653808), PE-conjugated FoxP3 (BioLegend #320008), and eFluor 780 fixable viability dye (eBioscience #65-0865-14) in separate panels. Samples were run on BD LSRII or BD LSR Fortessa flow cytometers and analyzed using FlowJo software.

**Cytokine Analysis of Scaffold Site:** Vaccine sites were explanted from immunized mice after sacrifice. PLG scaffolds were cut into <1 mm pieces using a razor blade and placed in Tissue Protein Extraction Reagent (T-PER, Fisher Scientific #PI78510) containing a protease inhibitor cocktail (Promega #G6521), vortexed, and sonicated. The solution was centrifuged at 13 000×g for 5 min and supernatant was collected and stored at −80 °C. A panel of cytokines (Bio-Plex Pro Mouse Cytokine Th1/Th2 Assay, BioRad #M6000003J7) was assessed using a BioPlex 3D system. Alternatively, IL-5 was assessed using an IL-5 ELISA kit (Invitrogen #88-7054-22).

**Cell Culture:** TUBO cells (HER2<sup>+</sup> breast cancer) were cloned from a spontaneous mammary tumor in a BALB/c neu-Tg mouse and were kindly provided by Dr. Yang-Xin Fu (University of Texas Southwestern Medical Center).<sup>[63,64]</sup> TUBO cells were cultured in Dulbecco's modified Eagle medium (DMEM) + 10% fetal bovine serum (FBS). 4T1 cells (ATCC, triple-negative mouse breast cancer) were cultured in DMEM + 10% FBS + 1% penicillin/xstreptomycin. Both were cultured at 37 °C with 5% CO<sub>2</sub>.

**Serum Binding Assay:** Mice were immunized with PLG vaccines against HER2 peptide and serum was collected at several timepoints. HER2<sup>+</sup> (TUBO) and HER2<sup>−</sup> (4T1) breast cancer cells were added to 96-well plates, blocked with anti-CD16/CD32 (eBiosciences #14-0161-81), and incubated with 1:100 diluted serum or trastuzumab as a positive control. After washing to remove unbound antibody, cells were incubated with PE-conjugated anti-mouse IgG (Invitrogen #P-852) and 7-AAD viability staining solution (Invitrogen #00-6993-50), run on a BD LSR Fortessa flow cytometer and analyzed using FlowJo software.

**Infectious Disease Model:** Mice were prophylactically vaccinated with PLG vaccines and challenged intraperitoneally with 5 × 10<sup>6</sup> colony forming units of RS218 *E. coli* as previously described.<sup>[26]</sup> Mice were monitored several times daily for mortality and humane criteria and euthanized when moribund. To determine organ bacterial burden, lungs, kidneys, liver, and spleen were collected, fragmented, and plated to quantify colony forming units.

**Statistical Analysis:** Statistical analyses were performed using GraphPad Prism v8 software. For normally distributed samples, analysis between two groups was performed using a two-tailed Student's *t*-test, or a Mann-Whitney U test otherwise. Multiple comparisons were conducted using a one-way analysis of variance (ANOVA) with Tukey's post hoc test when normally distributed, or a Kruskal-Wallis test with Dunn's post hoc test otherwise. All data are depicted as mean ± SD. Sample sizes of 4–10 biologically independent animals per group were used for in vivo studies, determined empirically based on results from prior publications along with approval from Harvard University's Institutional Animal Care and Use Committee.

## Supporting Information

Supporting Information is available from the Wiley Online Library or from the author.

## Acknowledgements

This work was supported by the National Institutes of Health/ National Cancer Institute (R01 CA223255) and the Wyss Institute for Biologically Inspired Engineering. A.J.N. acknowledges a Graduate Research Fellowship from the National Science Foundation. T.B.-R. acknowledges financial support from the European Union's Horizon 2020 research and innovation programme under the Marie Skłodowska-Curie grant agreement (No. 892758). The authors thank Beverly Lu and Catia Verbeke for advice, discussion, and data interpretation; Fernanda Langello and Mohan Karkada for coordinating RS218 experiments; and Shanda Lightbown for assisting with BioPlex operation.

## Conflict of Interest

D.J.M. declares the following competing interests: Novartis, sponsored research, licensed IP; Immulus, equity; IVIVA, SAB; Attivare, SAB, equity; Lyell, licensed IP, equity. E.J.D., C.D.Y., and B.T.S. are employed at Attivare Therapeutics. The other authors declare no competing interests.

## Data Availability Statement

The data that support the findings of this study are available from the corresponding author upon reasonable request.

## Keywords

antibodies, biomaterial scaffolds, germinal center, humoral response, single-shot vaccines

Received: October 27, 2021

Revised: December 18, 2021

Published online: January 8, 2022

- [1] S. W. Roush, T. V. Murphy, M. M. Basket, J. K. Iskander, J. S. Moran, J. F. Seward, A. Wasley, *J. Am. Med. Assoc.* **2007**, *298*, 2155.
- [2] X. Li, C. Mukandavire, Z. M. Cucunubá, S. E. Londono, K. Abbas, H. E. Clapham, M. Jit, H. L. Johnson, T. Papadopoulos, E. Vynnycky, M. Brisson, E. D. Carter, A. Clark, M. J. de Villiers, K. Eilertson, M. J. Ferrari, I. Gamkrelidze, K. A. M. Gaythorpe, N. C. Grassly, T. B. Hallett, W. Hinsley, M. L. Jackson, K. Jean, A. Karachaliou, P. Klepac, J. Lessler, X. Li, S. M. Moore, S. Nayagam, D. M. Nguyen, H. Razavi, D. Razavi-Shearer, S. Resch, C. Sanderson, S. Sweet, S. Sy, Y. Tam, H. Tanvir, Q. M. Tran, C. L. Trotter, S. Truelove, K. van Zandvoort, S. Verguet, N. Walker, A. Winter, K. Woodruff, N. M. Ferguson, T. Garske, *Lancet* **2021**, *397*, 398.
- [3] A. J. Pollard, E. M. Bijker, *Nat. Rev. Immunol.* **2021**, *21*, 83.
- [4] A. J. Najibi, D. J. Mooney, *Adv. Drug Delivery Rev.* **2020**, *161*, 42.
- [5] N. S. De Silva, U. Klein, *Nat. Rev. Immunol.* **2015**, *15*, 137.
- [6] R. L. Coffman, B. W. P. Seymour, D. A. Lebnan, D. D. Hiraki, J. A. Christiansen, B. Shrader, H. M. Cherwinski, H. F. J. Savelkoul, F. D. Finkelman, M. W. Bond, T. R. Mosmann, *Immunol. Rev.* **1988**, *102*, 5.
- [7] R. I. Nurieva, Y. Chung, *Cell. Mol. Immunol.* **2010**, *7*, 190.
- [8] K. Lederer, D. Castaño, D. Gómez Atria, T. H. Oguin, S. Wang, T. B. Manzoni, H. Muramatsu, M. J. Hogan, F. Amanat, P. Cherubin, K. A. Lundgreen, Y. K. Tam, S. H. Y. Fan, L. C. Eisenlohr, I. Maillard, D. Weissman, P. Bates, F. Krammer, G. D. Sempowski, N. Pardi, M. Locci, *Immunity* **2020**, *53*, 1281.
- [9] J. S. Turner, J. A. O. Halloran, E. Kalaidina, W. Kim, A. J. Schmitz, J. Q. Zhou, T. Lei, M. Thapa, R. E. Chen, J. B. Case, F. Amanat,

- A. M. Rauseo, A. Haile, X. Xie, M. K. Klebert, S. Teresa, D. Middleton, P. Shi, F. Krammer, S. A. Teefey, M. S. Diamond, R. M. Presti, A. H. Ellebedy, *Nature* **2021**.
- [10] K. J. McHugh, R. Guarecuco, R. Langer, A. Jaklenec, *J. Controlled Release* **2015**, 219, 596.
- [11] A. N. Chard, M. Gacic-Dobo, M. S. Diallo, S. V. Sodha, A. S. Wallace, *Morb. Mortal. Wkly. Rep.* **2020**, 69, 1706.
- [12] J. L. Kriss, L. E. Reynolds, A. Wang, S. Stokley, M. M. Cole, L. T. Q. Harris, L. K. Shaw, C. L. Black, J. A. Singleton, D. L. Fitter, D. A. Rose, M. D. Ritchey, R. L. Toblin, *MMWR Recomm. Rep.* **2021**, 70, 389.
- [13] M. G. Thompson, J. L. Burgess, A. L. Naleway, H. L. Tyner, S. K. Yoon, J. Meece, L. E. W. Olsho, A. J. Caban-Martinez, A. Fowlkes, K. Lutrick, J. L. Kuntz, K. Dunnigan, M. J. Odean, K. T. Hegmann, E. Stefanski, L. J. Edwards, N. Schaefer-Solle, L. Grant, K. Ellingson, H. C. Groom, T. Zunie, M. S. Thiese, L. Ivacic, M. G. Wesley, J. M. Lamberte, X. Sun, M. E. Smith, A. L. Phillips, K. D. Groover, Y. M. Yoo, J. Gerald, R. T. Brown, M. K. Herring, G. Joseph, S. Beitel, T. C. Morrill, J. Mak, P. Rivers, K. M. Harris, D. R. Hunt, M. L. Arvay, P. Kutty, A. M. Fry, M. Gaglani, *Morb. Mortal. Wkly. Rep.* **2021**, 70, 495.
- [14] G. Vidarsson, G. Dekkers, T. Rispens, *Front. Immunol.* **2014**, 5, 520.
- [15] J. M. Leal, J. Y. Huang, K. Kohli, C. Stoltzfus, M. R. Lyons-cohen, B. E. Olin, M. G. jr., M. Y. Gerner, **2021**, 9435, eabb9435.
- [16] D. Y. Tesfaye, A. Gudjonsson, B. Bogen, E. Fossum, *Front. Immunol.* **2019**, 10, 1529.
- [17] O. A. Ali, N. Huebsch, L. Cao, G. Dranoff, D. J. Mooney, *Nat. Mater.* **2009**, 8, 151.
- [18] A. W. Li, M. C. Sobral, S. Badrinath, Y. Choi, A. Graveline, A. G. Staffier, J. C. Weaver, M. O. Dellacherie, T. Y. Shih, O. A. Ali, J. Kim, K. W. Wucherpennig, D. J. Mooney, *Nat. Mater.* **2018**, 17, 528.
- [19] I. Preis, R. S. Langer, *J. Immunol. Methods* **1979**, 28, 193.
- [20] K. M. Cirelli, S. Crotty, *Curr. Opin. Immunol.* **2017**, 47, 64.
- [21] M. Allahyari, E. Mohit, *Hum. Vaccines Immunother.* **2016**, 12, 806.
- [22] K. Adu-Berchie, D. J. Mooney, *Acc. Chem. Res.* **2020**, 53, 1749.
- [23] M. O. Dellacherie, B. R. Seo, D. J. Mooney, *Nat. Rev. Mater.* **2019**, 4, 379.
- [24] O. A. Ali, D. Emerich, G. Dranoff, D. J. Mooney, *Sci. Transl. Med.* **2009**, 8ra19.
- [25] M. O. Dellacherie, A. Li, B. Y. Lu, C. S. Verbeke, L. Gu, A. G. Stafford, E. J. Doherty, D. J. Mooney, *Adv. Funct. Mater.* **2020**, 30, 2002448.
- [26] M. Super, E. J. Doherty, M. J. Cartwright, B. T. Seiler, F. Langellotto, N. Dimitrakakis, D. A. White, A. G. Stafford, M. Karkada, A. R. Graveline, C. L. Horgan, K. R. Lightbown, F. R. Urena, C. D. Yeager, S. A. Rifai, M. O. Dellacherie, A. W. Li, C. Leese-thompson, H. Ijaz, A. R. Jiang, V. Chandrasekhar, J. M. Scott, S. L. Lightbown, D. E. Ingber, D. J. Mooney, *Nat. Biomed. Eng.* **2021**, 2157.
- [27] P. J. Delves, T. Lund, I. M. Roitt, *Trends Immunol.* **2002**, 23, 213.
- [28] F. F. Aguilar, J. J. Barranco, E. B. Fuentes, L. C. Aguilera, Y. L. Sáez, M. D. C. Santana, E. P. Vázquez, R. B. Baker, O. R. Acosta, H. G. Pérez, G. G. Nieto, *Vaccine* **2012**, 30, 6595.
- [29] M. S. Simms, D. P. Scholfield, E. Jacobs, D. Michaeli, P. Broome, J. E. Humphreys, M. C. Bishop, *Br. J. Cancer* **2000**, 83, 443.
- [30] J. Walker, S. Ghosh, J. Pagnon, C. Colantoni, A. Newbold, W. Zeng, D. C. Jackson, *Vaccine* **2007**, 25, 7111.
- [31] J. Kim, W. A. Li, Y. Choi, S. A. Lewin, C. S. Verbeke, G. Dranoff, D. J. Mooney, *Nat. Biotechnol.* **2015**, 33, 64.
- [32] T. Y. Shih, S. O. Blacklow, A. W. Li, B. R. Freedman, S. Bencherif, S. T. Koshy, M. C. Darnell, D. J. Mooney, *Adv. Healthcare Mater.* **2018**, 7, 1701469.
- [33] S. A. Bencherif, R. W. Sands, O. A. Ali, W. A. Li, S. A. Lewin, T. M. Braschler, T. Y. Shih, C. S. Verbeke, D. Bhatta, G. Dranoff, D. J. Mooney, *Nat. Commun.* **2015**, 6, 7556.
- [34] A. M. Collins, *Immunol. Cell Biol.* **2016**, 94, 949.
- [35] Z. Zhang, T. Goldschmidt, H. Salter, *Mol. Immunol.* **2012**, 50, 169.
- [36] Y. Hamaguchi, Y. Xiu, K. Komura, F. Nimmerjahn, T. F. Tedder, *J. Exp. Med.* **2006**, 203, 743.
- [37] A. Jegerlehner, P. Maurer, J. Bessa, H. J. Hinton, M. Kopf, M. F. Bachmann, *J. Immunol.* **2007**, 178, 2415.
- [38] J. T. Garrett, S. Rawale, S. D. Allen, G. Phillips, G. Forni, J. C. Morris, P. T. P. Kaumaya, *J. Immunol.* **2007**, 178, 7120.
- [39] M. Achtman, A. Mercer, B. Kusecek, A. Pohl, M. Heuzenroeder, W. Aaronson, A. Sutton, R. P. Silver, *Infect. Immun.* **1983**, 39, 315.
- [40] R. P. Silver, W. Aaronson, A. Sutton, R. Schneerson, *Infect. Immun.* **1980**, 29, 200.
- [41] H. H. Tam, M. B. Melo, M. Kang, J. M. Pelet, V. M. Ruda, M. H. Foley, J. K. Hu, S. Kumari, J. Crampton, A. D. Baldeon, R. W. Sanders, J. P. Moore, S. Crotty, R. Langer, D. G. Anderson, A. K. Chakraborty, D. J. Irvine, *Proc. Natl. Acad. Sci. USA* **2016**, 113, E6639.
- [42] B. J. Kwee, B. R. Seo, A. J. Najibi, A. W. Li, T. Y. Shih, D. White, D. J. Mooney, *Sci. Adv.* **2019**, 5, eaav6313.
- [43] P. Bruhns, F. Jönsson, *Immunol. Rev.* **2015**, 268, 25.
- [44] R. Stewart, S. A. Hammond, M. Oberst, R. W. Wilkinson, *J. Immunother. Cancer* **2014**, 2, 29.
- [45] G. A. Roth, O. M. Saouaf, A. A. A. Smith, E. C. Gale, M. A. Hernandez, J. Idoyaga, E. A. Appel, *ACS Biomater. Sci. Eng.* **2021**, 7, 1889.
- [46] L. Lin, A. J. Gerth, S. L. Peng, *Eur. J. Immunol.* **2004**, 34, 1483.
- [47] F. Wegmann, K. H. Gartlan, A. M. Harandi, S. A. Brinckmann, M. Coccia, W. R. Hillson, W. L. Kok, S. Cole, L. P. Ho, T. Lambe, M. Puthia, C. Svanborg, E. M. Scherer, G. Krashias, A. Williams, J. N. Blattman, P. D. Greenberg, R. A. Flavell, A. E. Moghaddam, N. C. Sheppard, Q. J. Sattentau, *Nat. Biotechnol.* **2012**, 30, 883.
- [48] C. C. Dai, J. Yang, W. M. Hussein, L. Zhao, X. Wang, Z. G. Khalil, R. J. Capon, I. Toth, R. J. Stephenson, *ACS Infect. Dis.* **2020**, 6, 2502.
- [49] N. C. Sheppard, S. A. Brinckmann, K. H. Gartlan, M. Puthia, C. Svanborg, G. Krashias, S. C. Eisenbarth, R. A. Flavell, Q. J. Sattentau, F. Wegmann, *Int. Immunol.* **2014**, 26, 531.
- [50] Y. Srisomboon, N. Ohkura, K. Iijima, T. Kobayashi, P. J. Maniak, H. Kita, S. M. O'grady, *Int. J. Mol. Sci.* **2021**, 22.
- [51] V. Mulens-Arias, J. M. Rojas, S. Pérez-Yagüe, M. P. Morales, D. F. Barber, *Biomaterials* **2015**, 52, 494.
- [52] M. I. Harrell, B. M. Iritani, A. Ruddle, *J. Immunol. Methods* **2008**, 332, 170.
- [53] G. A. Roth, E. C. Gale, M. Alcantara-Hernandez, W. Luo, E. Axpe, R. Verma, Q. Yin, A. C. Yu, H. L. Hernandez, C. L. Maikawa, A. A. A. Smith, M. M. Davis, B. Pulendran, J. Idoyaga, E. A. Appel, *ACS Cent. Sci.* **2020**, 6, 1800.
- [54] C. A. Hudis, *N. Engl. J. Med.* **2007**, 357, 39.
- [55] B. Petricevic, J. Laengle, J. Singer, M. Sachet, J. Fazekas, G. Steger, R. Bartsch, E. Jensen-Jarolim, M. Bergmann, *J. Transl. Med.* **2013**, 11, 307.
- [56] R. Gennari, S. Menard, F. Fagnoni, L. Ponchio, M. Scelsi, E. Tagliabue, F. Castiglioni, L. Villani, C. Magalotti, N. Gibelli, B. Oliviero, B. Ballardini, G. D. Prada, A. Zambelli, A. Costa, *Clin. Cancer Res.* **2004**, 10, 5650.
- [57] M. M. Xu, Y. Pu, Y. Zhang, Y. X. Fu, *Trends Immunol.* **2016**, 37, 141.
- [58] S. L. Demento, A. L. Siefert, A. Bandyopadhyay, F. A. Sharp, T. M. Fahmy, *Trends Biotechnol.* **2011**, 29, 294.
- [59] T. H. Mogensen, *Clin. Microbiol. Rev.* **2009**, 22, 240.
- [60] M. F. Bachmann, G. T. Jennings, *Nat. Rev. Immunol.* **2010**, 10, 787.
- [61] H. Iida, T. Takai, Y. Hirasawa, S. Kamijo, S. Shimura, H. Ochi, I. Nishioka, N. Maruyama, H. Ogawa, K. Okumura, S. Ikeda, *Allergol. Int.* **2014**, 63, 219.
- [62] M. Hirose, A. Recke, T. Beckmann, A. Shimizu, A. Ishiko, K. Bieber, J. Westermann, D. Zillikens, E. Schmidt, R. J. Ludwig, *J. Immunol.* **2011**.
- [63] S. G. Park, Z. Jiang, E. D. Mortenson, L. Deng, O. Radkevich-Brown, X. Yang, H. Sattar, Y. Wang, N. K. Brown, M. Greene, Y. Liu, J. Tang, S. Wang, Y. X. Fu, *Cancer Cell* **2010**, 18, 160.
- [64] S. Rovero, A. Amici, E. Di Carlo, R. Bei, P. Nanni, E. Quagliano, P. Porcedda, K. Boggio, A. Smorlesi, P.-L. Lollini, L. Landuzzi, M. P. Colombo, M. Giovarelli, P. Musiani, G. Forni, *J. Immunol.* **2000**, 165, 5133.